Applied Physics Express

LETTERS

Electrical contacts to thin layers of $Bi_2Sr_2CaCu_2O_{8+\delta}$

To cite this article: Shota Suzuki *et al* 2018 *Appl. Phys. Express* **11** 053201

Applied Physics Express **11**, 053201 (2018)
https://doi.org/**10.7567/APEX.11.053201**

Electrical contacts to thin layers of $Bi_2Sr_2CaCu_2O_{8+\delta}$

Shota Suzuki[1], Hiroki Taniguchi[1], Tsukasa Kawakami[1], Maxen Cosset-Cheneau[1], Tomonori Arakawa[1,2], Shigeki Miyasaka[1], Setsuko Tajima[1], Yasuhiro Niimi[1,2]*, and Kensuke Kobayashi[1,2]

[1]*Department of Physics, Graduate School of Science, Osaka University, Toyonaka, Osaka 560-0043, Japan*
[2]*Center for Spintronics Research Network, Osaka University, Toyonaka, Osaka 560-8531, Japan*

*E-mail: niimi@phys.sci.osaka-u.ac.jp

Received March 16, 2018; accepted April 10, 2018; published online April 26, 2018

Thin layers of $Bi_2Sr_2CaCu_2O_{8+\delta}$ (Bi2212) were fabricated using the mechanical exfoliation technique. Good electrical contacts to the thin Bi2212 films with low contact resistance were realized by depositing Ag and Au electrodes onto the Bi2212 films and annealing them with an oxygen flow at 350 °C for 30 min. We observed cross-section images of the Bi2212 thin film device using a transmission electron microscope to characterize the diffusion of Ag and Au atoms into the Bi2212 thin film. © 2018 The Japan Society of Applied Physics

Two-dimensional (2D) atomic crystals have attracted much attention from the perspective of both fundamental research and practical application.[1,2] Graphene, a single layer of graphite, is a pioneering material that has been studied in a variety of experiments, such as investigations of the quantum Hall effect[3–6] and spin transport measurements.[7–9] Transition metal dichalcogenides (TMDs) have also been fabricated into 2D layers.[1,2] For instance, MoS_2 is inherently semiconducting, but by applying an electric field to an atomically thin MoS_2 film, the carrier density in the film is increased, which results in metallic behavior[10] and eventually superconductivity at low temperatures.[11]

As demonstrated for graphene[3–6] and TMDs,[10,11] electric field effects are expected for a variety of atomically thin films.[1,2] The motivation for the present study is the electric field effect for high-T_c (critical temperature) superconductors. In high-T_c superconductors, carrier doping has been achieved by chemical substitution[12] and/or oxygen doping.[13,14] If reversible carrier doping is realized by the electric field effect, a wide doping range from the underdoped region to the overdoped region via the optimum T_c condition can be investigated in one atomically-thin high-T_c superconductor device simply by tuning the electric field. This could be helpful for understanding the detailed mechanism of high-T_c superconductors. However, there have been relatively few experimental studies on thin layers of high-T_c superconductors,[15–17] compared with those on TMDs. One of the issues associated with the realization of thin-layer high-T_c superconductor devices is the difficulty of fabricating good electrical contacts to them.

In this study, we present a method to obtain electrical contacts to thin films of $Bi_2Sr_2CaCu_2O_{8+\delta}$ (Bi2212), a cleavable high-T_c superconductor, using the mechanical exfoliation technique (commonly known as the "scotch tape" technique).[1] We also show how the electrical contacts can be realized by observing cross-sectional images of the thin film device with a transmission electron microscope (TEM). Such thin layers of Bi2212 can be integrated into future 2D circuits made of graphene and hexagonal boron nitride,[18,19] where all functions could be tuned by applying an electric field.

Single-crystalline Bi2212 was grown by the floating zone method.[20,21] The crystal structure of Bi2212 is shown in Fig. 1(a). Because the interaction between the two BiO layers is weak, the exfoliation takes place between the two BiO layers. The excess oxygen atoms are also added between the two BiO layers. Conversely, superconductivity arises at the CuO layer.

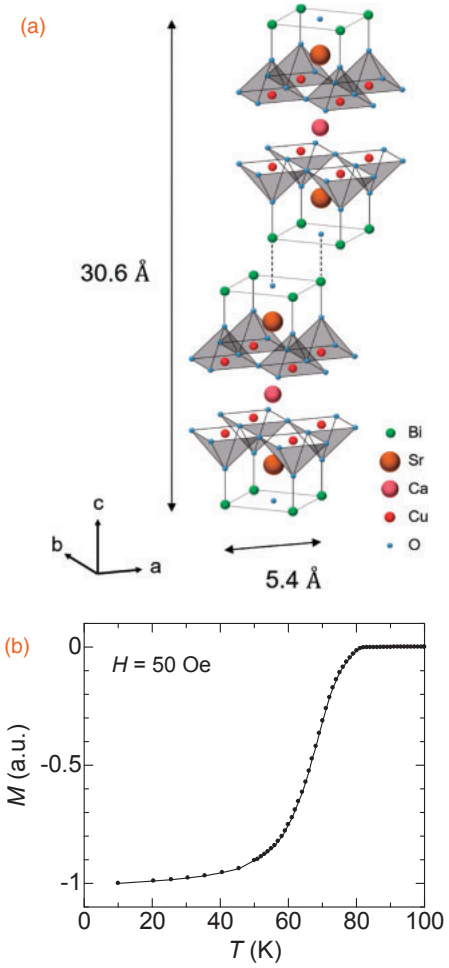

Fig. 1. (a) Crystal structure of Bi2212. The lattice constants along the *a*- and *c*-axes are 5.4 and 30.6 Å, respectively. (b) Temperature dependence of magnetization M (normalized at $T = 10$ K) for the overdoped Bi2212 bulk sample used in the present work. The applied magnetic field H is 50 Oe. T_c of the overdoped Bi2212 is determined to be 80 K.

To prevent the escape of oxygen from the Bi2212 crystal, which reduces the carrier density, during the mechanical exfoliation and lithography processes, we chose an overdoped Bi2212, where the hole doping p is approximately 0.2.[22] The overdoped Bi2212 was obtained by annealing the crystal at 700 °C for 1 week in a flow of O_2 gas. The magnetization M of the overdoped Bi2212 is shown in Fig. 1(b). T_c of the

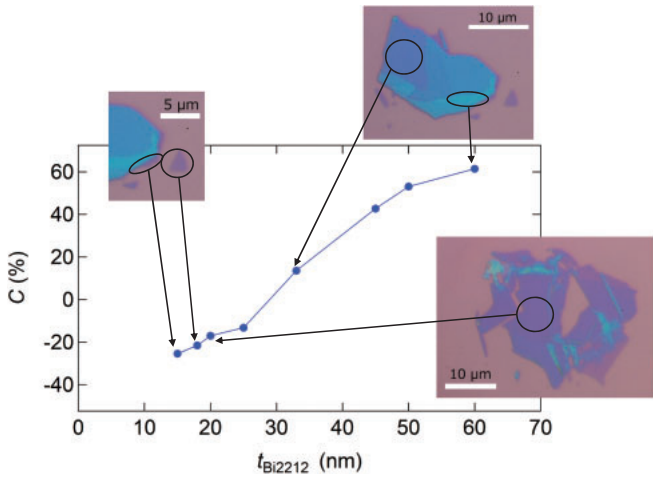

Fig. 2. Green contrast ratio C (defined in the text) for various Bi2212 film thicknesses. Typical optical microscope images are also shown in the figure.

bulk sample is estimated to be 80 K from the magnetization measurement.

We then performed standard mechanical exfoliation for the overdoped Bi2212 under ambient conditions. After repeating the exfoliation process, a scotch tape with many Bi2212 flakes was pasted onto a SiO_2 (285 nm)/Si substrate with several 100 nm thick gold marks. Typical optical microscope images of Bi2212 films with various thicknesses are shown in Fig. 2. To determine the thickness of Bi2212 from the color of the film under the microscope, we measured the thickness of the film with a commercially available atomic force microscope (AFM) to obtain the relationship between the thickness and the color of the Bi2212 film. As detailed in Ref. 23, only the green intensity I of the reflected light was extracted from the optical microscope image. We then compared I of the SiO_2/Si substrate (I_{sub}) with I of the Bi2212 film on the substrate (I_{film}). By calculating the contrast ratio $C = (I_{film} - I_{sub})/I_{sub}$, we can relate C to the thickness of the film, as shown in Fig. 2.

To perform transport measurements, electrodes were attached to the thin films of Bi2212 using standard electron beam lithography and a subsequent lift-off process. A poly(methyl methacrylate) (PMMA) resist was coated on the substrate and dried in a vacuum box. To prevent the escape of oxygen from the Bi2212 thin films, we avoided heating the substrate to dry the resist. We then performed electron beam lithography, irradiating the PMMA resist with an electron beam. After the development of the resist, 50 nm thick Ag and Au electrodes were deposited by a Joule heating evaporator without breaking the vacuum.

We attempted the use of four different electrodes (Au/Ti, Au, Cu, and Au/Ag) to make electrical contact with the thin films of Bi2212. However, none of them presented good electrical contact with low contact resistance. Thus, we baked the Bi2212 device with Au/Ag electrodes at 350 °C for 30 min with an O_2 gas flow,[24] as previously demonstrated for micro-meter-scale high-T_c superconductor devices.[25] For bulk Bi2212 samples, electrical contacts were achieved by annealing as-grown Bi2212 with Au paste at 600–800 °C.[21] However, this high-temperature annealing decomposed the thin Bi2212 films. Thus, we decreased the annealing temperature gradually and found that annealing at 350 °C for 30 min can achieve electrical contacts to the Bi2212 films with low contact resistance. The contact resistance was approximately 100 Ω for an area of 10 μm^2, which is comparable to those for TMDs and Au/Ti electrodes.[26]

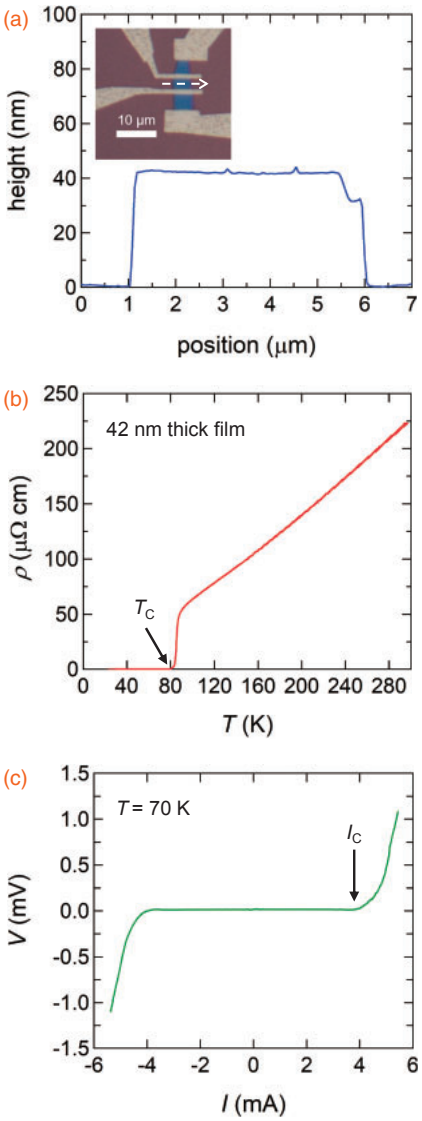

Fig. 3. (a) Cross section of Bi2212 film measured with the AFM. The inset shows an optical microscope image of the device. The cross section is taken along the dotted arrow in the inset. (b) Resistivity ρ of the 42 nm thick Bi2212 device as a function of temperature T. T_c is the same as that of the bulk sample. (c) I–V characteristics for the same device as in (b). The critical current of this device is 4 mA.

Figure 3(a) shows an optical microscope image of a typical Bi2212 thin film device. From the AFM image, the thickness of the Bi2212 is estimated to be 42 nm. In Fig. 3(b), we present the temperature dependence of the resistivity of the 42 nm thick Bi2212 device. With decreasing temperature, the resistivity decreases almost linearly, but with a slight convex downward behavior [i.e., T^n $(n > 1)$], which shows the superconducting transition at 80 K, typical of overdoped Bi2212.[21,27,28] To further characterize the Bi2212 thin film, we measured current–voltage (I–V) curves at temperatures just below T_c. As shown in Fig. 3(c), the critical current is approximately 4 mA at $T = 70$ K. The critical current density J_c reaches 2×10^{10} A/m^2. Thus, a much larger critical current density can be expected at lower temperatures.

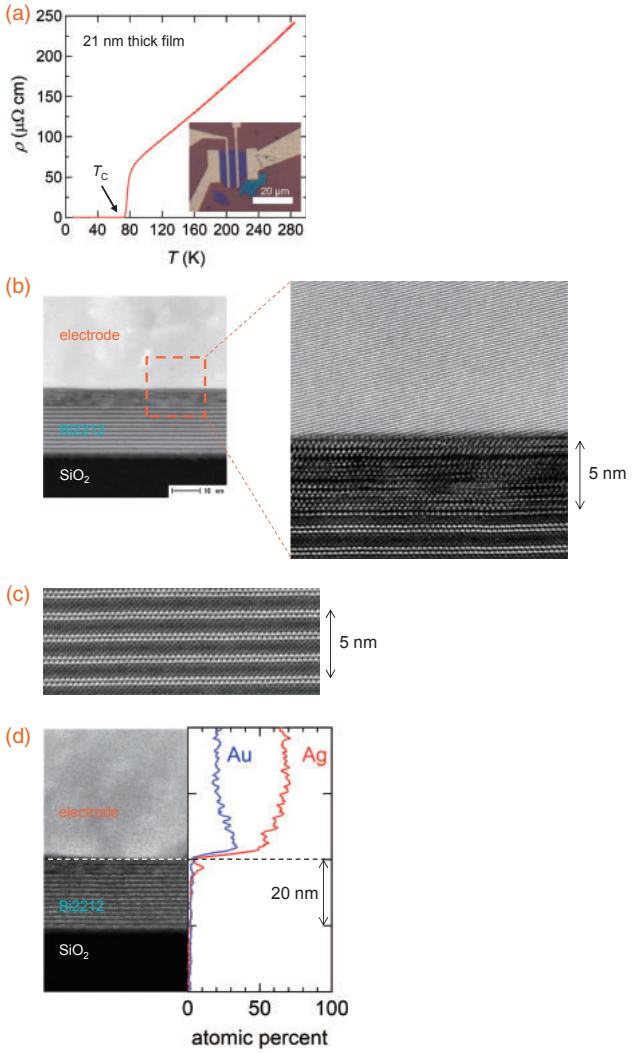

Fig. 4. (a) Resistivity ρ of a 21-nm-thick Bi2212 device as a function of temperature T. The inset shows an optical microscope image of the device. (b, c) HAADF-STEM images taken in the vicinity of and far from the Au/Ag electrode, respectively. The right figure in (b) is a magnified image of the broken-line area in the left figure. (d) EDX line profiles taken in the same area as the left HAADF-STEM image with Ag and Au L-lines.

As mentioned above, the key issue for realizing Bi2212 devices is obtaining good electrical contacts with thin Bi2212 films. To gain information concerning the interface between the Bi2212 and the Au/Ag electrodes, we obtained a cross-sectional image of a 21-nm-thick Bi2212 device using TEM. Even for the 21-nm-thick device, a clear superconducting transition can be observed, as shown in Fig. 4(a), although T_c (= 73 K) is slightly lower than that of the 42-nm-thick device. Figures 4(b) and 4(c) show high-angle annular dark field scanning TEM (HAADF-STEM) images taken in the vicinity of and far from the Au/Ag electrode, respectively. The brightest white spheres correspond to Bi atoms. The Bi atoms are regularly arranged far from the electrode in Fig. 4(c). Conversely, it is clear that there is an intermediate layer 5 nm in thickness between the Au/Ag electrode and Bi2212 in Fig. 4(b). As can be seen in the right panel of Fig. 4(b), the Bi atoms are not regularly arranged immediately below the electrode, but such irregularity is suppressed at approximately 5 nm from the interface, and the regular arrangement of Bi atoms is maintained below this depth.

To characterize the diffusion of Ag and Au atoms into the Bi2212, we performed energy dispersive X-ray (EDX) analysis of the electrode/Bi2212 junction. In Fig. 4(d), we show the EDX line profiles for Ag and Au atoms near the interface between the Au/Ag electrode and the Bi2212 film. Apparently, the Ag and Au atoms the Ag and Au atoms in the electrode are mixed up after annealing after annealing. A small amount of Ag atoms diffuse into the Bi2212 thin layer, within 5 nm from the interface. The maximum distribution of Ag is at approximately 2–3 nm from the interface between Au/Ag and Bi2212 and is suppressed beyond 5 nm. Considering all of the possible elements (Bi, Sr, Ca, Cu, O, Au, and Ag), the maximum percentage of Ag in the diffusion area is approximately 10%. This fact has never been reported so far. However, Au does not diffuse into the Bi2212 thin film. This experimental fact clearly shows that the diffusion of Ag atoms into Bi2212 is essential to obtain a good electrical contact with thin layers of Bi2212.

In summary, we have fabricated thin layers of Bi2212 using the mechanical exfoliation technique. Electrical contact with Bi2212 films was realized by depositing Ag and Au without breaking vacuum and annealing the devices at 350 °C for 30 min with a flow of O_2 gas. T_c of the Bi2212 thin films is almost the same as that of the bulk material. Analysis of the Bi2212 device with cross-sectional TEM images and EDX suggest that the diffusion of Ag atoms by 5 nm from the interface between the electrode and Bi2212 is essential to obtain good electrical contact with Bi2212. This result is the first step toward integration of high-T_c superconductors into 2D atomic-layer circuits.

Acknowledgment This work was supported by Grants-in-Aid for Scientific Research (Nos. JP16H05964, JP17K18756, JP26103002, JP26220711, and JP15K17680), Mazda Foundation, Shimadzu Science Foundation, Yazaki Foundation, SCAT Foundation, and Murata Foundation.

1) K. S. Novoselov, D. Jiang, F. Schedin, T. J. Booth, V. V. Khotkevich, S. V. Morozov, and A. K. Geim, Proc. Natl. Acad. Sci. U.S.A. **102**, 10451 (2005).
2) A. K. Geim and I. V. Grigorieva, Nature **499**, 419 (2013).
3) K. S. Novoselov, A. K. Geim, S. V. Morozov, D. Jiang, Y. Zhang, S. V. Dubonos, I. V. Grigorieva, and A. A. Firsov, Science **306**, 666 (2004).
4) K. S. Novoselov, A. K. Geim, S. V. Morozov, D. Jiang, M. I. Katsnelson, I. V. Grigorieva, S. V. Dubonos, and A. A. Firsov, Nature **438**, 197 (2005).
5) Y. Zhang, Y.-W. Tan, H. L. Stormer, and P. Kim, Nature **438**, 201 (2005).
6) A. H. Castro Neto, F. Guinea, N. M. R. Peres, K. S. Novoselov, and A. K. Geim, Rev. Mod. Phys. **81**, 109 (2009).
7) N. Tombros, C. Jozsa, M. Popinciuc, H. T. Jonkman, and B. J. van Wees, Nature **448**, 571 (2007).
8) W. Han, K. Pi, K. M. McCreary, Y. Li, J. J. I. Wong, A. G. Swartz, and R. K. Kawakami, Phys. Rev. Lett. **105**, 167202 (2010).
9) W. Han, R. K. Kawakami, M. Gmitra, and J. Fabian, Nat. Nanotechnol. **9**, 794 (2014).
10) B. Radisavljevic, A. Radenovic, J. Brivio, V. Giacometti, and A. Kis, Nat. Nanotechnol. **6**, 147 (2011).
11) J. T. Ye, Y. J. Zhang, R. Akashi, M. S. Bahramy, R. Arita, and Y. Iwasa, Science **338**, 1193 (2012).
12) H. Takagi, R. J. Cava, M. Marezio, B. Batlogg, J. J. Krajewski, W. F. Peck, Jr., P. Bordet, and D. E. Cox, Phys. Rev. Lett. **68**, 3777 (1992).
13) K. Kishio, J. Shimoyama, T. Hasegawa, K. Kitazawa, and K. Fueki, Jpn. J. Appl. Phys. **26**, L1228 (1987).
14) Y. Yamada, T. Watanabe, and M. Suzuki, Physica C **460–462**, 815 (2007).
15) X. Wang, L. X. You, D. K. Liu, C. T. Lin, X. M. Xie, and M. H. Jiang, Physica C **474**, 13 (2012).
16) D. Jiang, T. Hu, L. You, Q. Li, A. Li, H. Wang, G. Mu, Z. Chen, H. Zhang, G. Yu, J. Zhu, Q. Sun, C. Lin, H. Xiao, X. Xie, and M. Jiang, Nat. Commun. **5**, 5708 (2014).
17) A. Jindal, D. A. Jangade, N. Kumar, J. Vaidya, I. Das, R. Bapat, J. Parmar,

B. A. Chalke, A. Thamizhavel, and M. M. Deshmukh, Sci. Rep. **7**, 3295 (2017).
18) C. R. Dean, A. F. Young, I. Meric, C. Lee, L. Wang, S. Sorgenfrei, K. Watanabe, T. Taniguchi, P. Kim, K. L. Shepard, and J. Hone, Nat. Nanotechnol. **5**, 722 (2010).
19) L. A. Ponomarenko, A. K. Geim, A. A. Zhukov, R. Jalil, S. V. Morozov, K. S. Novoselov, I. V. Grigorieva, E. H. Hill, V. V. Cheianov, V. I. Fal'ko, K. Watanabe, T. Taniguchi, and R. V. Gorbachev, Nat. Phys. **7**, 958 (2011).
20) G. D. Gu, K. Takamuku, N. Koshizuka, and S. Tanaka, J. Cryst. Growth **130**, 325 (1993).
21) H. Hobou, S. Ishida, K. Fujita, M. Ishikado, K. M. Kojima, H. Eisaki, and S. Uchida, Phys. Rev. B **79**, 064507 (2009).
22) We confirmed that for the optimum doping T_c was 92 K.
23) P. Blake, E. W. Hill, A. H. Castro Neto, K. S. Novoselov, D. Jiang, R. Yang, T. J. Booth, and A. K. Geim, Appl. Phys. Lett. **91**, 063124 (2007).
24) We have not tried only the Ag electrode to take an electrical contact. However, the Ag electrode would make AgO during the annealing process and thus the Au layer capping would be helpful to take good electrical contacts with low contact resistance.
25) Y. Yamada, K. Anagawa, T. Shibauchi, T. Fujii, T. Watanabe, A. Matsuda, and M. Suzuki, Phys. Rev. B **68**, 054533 (2003).
26) A. Allain, J. Kang, K. Banerjee, and A. Kis, Nat. Mater. **14**, 1195 (2015).
27) T. Watanabe, T. Fujii, and A. Matsuda, Phys. Rev. Lett. **79**, 2113 (1997).
28) H. Takagi, B. Batlogg, H. L. Kao, J. Kwo, R. J. Cava, J. J. Krajewski, and W. F. Peck, Jr., Phys. Rev. Lett. **69**, 2975 (1992).